Quantifying Rock Glacier Creep Using Airborne Laser Scanning: A Case Study from Two Rock Glaciers in the Austrian Alps

Erik Bollmann, Christoph Klug, Rudolf Sailer, Johann Stötter
Institute of Geography, Innsbruck University, Innsbruck, Austria

Jakob Abermann
Institute of Meteorology and Geophysics, Innsbruck University, Innsbruck, Austria

Abstract

Horizontal displacement rates as well as surface elevation changes of two rock glaciers in the Eastern Austrian Alps are calculated over different time spans between 2006 and 2010 using airborne laser scanning (ALS) data and the image correlation software Imcorr. By comparing the ALS-based horizontal displacement rates with results from global navigation satellite system data (dGNSS), an average absolute deviation of 0.22 m (STD 0.30 m) is determined for the time period 2009–2010 and 0.34 m (STD 0.5 m) for 2006–2010. For the Äußere Hochebenkar rock glacier (AHK), a gradual increase of flow velocity from about 0.1 ma^{-1} at the root zone to > 2 ma^{-1} at the lower part is calculated for the period 2006–2010. Over the period 2009–2010, the velocity of AHK generally increased compared to 2006–2009. At the Kaiserberg rock glacier (KBR), two distinct flow velocity fields are detected. In contrast to AHK, the Kaiserberg rock glacier shows significant surface lowering caused by ice melt.

Keywords: accuracy; airborne laser scanning; creep; monitoring; permafrost; rock glacier; velocity.

Introduction

Active rock glaciers are morphological features composed of a mixture of ice and debris that slowly creep downslope by the force of gravity. As a consequence of the downslope movement, they show a typical surface topography with transverse and longitudinal ridges and furrows, a steep front, and lateral sides (Barsch 1996). The surface topography is the result of an interaction between mass advection, advection of topography by creep, 3-dimensional strain, and local mass changes (Barsch 1996, Kääb et al. 2003), and it cumulatively reflects the dynamic history and thus the past and present internal conditions of the rock glacier (Kääb & Weber 2004).

Active rock glaciers creep with surface velocities ranging from a few centimeters to several meters per year. The majority of them show surface velocities around one meter per year or below (Haeberli 1985, Whalley & Martin 1992, Barsch 1996, Kaufmann & Landstädter 2003, Haeberli et al. 2006, Kääb 2007, Kääb et al. 2003). There are clear indications that differences in thickness, temperature, and internal composition play a major role in the deformation rate of rock glaciers. However, it is suggested that these factors do not sufficiently explain differences in velocity fields on individual rock glaciers (Kääb et al. 2003).

Within the last decade, an increasing number of studies monitored and quantified the creep of active rock glaciers. The main focus of recent research has been on either a better understanding of rock glacier evolution and kinetics (Kääb et al. 2003, Kääb & Weber 2004, Kääb & Reichmuth 2005, Roer et al. 2005), on an interpretation of surface velocity fields in relation to climatic and paleoclimatic conditions, or on rock glacier age estimations (Schneider & Schneider 2001, Kääb et al. 2002, Kääb et al. 2007).

To quantify 2- and 3-dimensional creep, various monitoring techniques have been applied. The potential of airborne laser scanning (ALS) for rock glacier studies, especially for volume change calculations, has already been mentioned by Harris et al. (2009). However, the volume change of a rock glacier, as it can be derived from multi-temporal Digital Terrain Model (DTM) differencing, only represents the results of an interaction between mass advection, advection of topography by creep, 3-dimensional straining, and local mass changes. To get a more detailed understanding of the processes involved in rock glacier creep, it is of fundamental interest to determine 3-dimensional surface displacement rates (Kääb & Weber 2004, Kääb & Reichmuth 2005).

In this contribution, horizontal displacement rates and vertical changes of two rock glaciers are calculated using multi-temporal ALS data. The accuracy of the results is assessed using differential global navigation satellite systems (dGNSS) data, and we discuss the potential of ALS for rock glacier analysis.

Monitoring Techniques

Established techniques for rock glacier monitoring

Today, a variety of methods to quantify rock glacier creep rates is available. Terrestrial survey techniques such as dGNSS are widely used. They provide highly accurate measurements over relatively long time series and high temporal resolution (Schneider & Schneider 2001, Krainer & Mostler 2006). Recently, terrestrial laser scanning grew in importance because it produces very high resolution digital terrain models and it can be applied over relatively large areas of a rock glacier (Bauer et al. 2003). The main disadvantage of the terrestrial surveys is the lack of area-wide data coverage. For area-wide data acquisition, airborne and space-borne monitoring techniques are more appropriate. Using photogrammetry on repeated

airborne optical data, highly accurate horizontal velocity fields and their spatio-temporal changes have been measured over entire rock glaciers (Kääb et al. 1997, Kaufmann & Landstädter 2003, Kääb et al., 2003, Kääb & Weber 2004, Roer et al. 2005). Space-borne radar interferometry has been successfully applied to detect and quantify surface deformation over large areas on rock glaciers (Kenny & Kaufmann 2003, Strozzi et al. 2004).

Airborne laser scanning (ALS)

ALS is an active remote-sensing technique, using a laser beam as the sensing carrier, for the acquisition of 3-dimensional point data that geometrically represent the earth surface or objects on it. In contrast to optical remote sensing raster data, the raw product of an ALS data acquisition campaign is a so-called point cloud consisting of points with x,y,z coordinates (Baltsavias 1999). Over the last 15 years, airborne laser scanning has become a standard method for the acquisition of high-resolution and high-accuracy topographic data. The accuracy of ALS-derived DTMs has been determined in several studies, and an absolute vertical accuracy in the order of one decimeter is given for areas less inclined than 30° (Baltsavias 1999, Hodgson & Bresnahan 2004, Bollmann et al. 2010).

Study Area and Data

Äußerer Hochebenkar rock glacier (AHK)

The Äußere Hochebenkar rock glacier is a tongue-shaped, talus-derived rock glacier in the Ötztal Alps, Austria. It expands from about 2830 m a.s.l. down to about 2365 m a.s.l. and reaches a length of 1.6 km. The surface layer is characterized by large boulders with an average diameter of about 1 m (Vietoris 1972, Haeberli & Patzelt 1982).

Systematic investigations on surface flow velocities, front advance rates, and surface elevation changes of AHK started in 1938 and have been carried out on at least an annual scale since then (Schneider & Schneider 2001). AHK is characterized by very high surface velocities of up to several meters per year in its lower part, especially below a terrain edge at about 2570 m. At the cross profile L1 (see Fig. 2), mean displacement rates of 3.9 ma^{-1} and maximum values of 6.6 ma^{-1} were recorded in the 1950s and 1960s (Schneider & Schneider 2001). These high values most likely resulted from sliding processes of the creeping permafrost body on the underlying bedrock (Haeberli & Patzelt 1982, Schneider & Schneider 2001).

Kaiserberg rock glacier (KBR)

The Kaiserberg rock glacier is a lobate rock glacier in the Ötztal Alps with a maximum width of about 550 m and a length of 350–400 m. The highest point at the rock glacier head is at 2710 m a.s.l. Following Krainer & Mostler (2006), the lowermost part of the rock glacier is active and ends with a steep front at an altitude of 2585 m a.s.l. KBR consists of a coarse-grained surface layer with blocks of several meters in length. However, most are several decimeters in diameter. The surface topography is characterized by well-developed transverse and longitudinal ridges and furrows.

Table 1. Overview of data acquisition dates.

Data acquisition dates		2006	2009	2010
ALS	AHK	23.08.	30.09.	07.10.
	KBR	02.09.	---	07.10.
dGNSS	AHK	22.09.	06.08.	08.09.
	KBR	---	---	---

ALS data

ALS data acquisition campaigns at AHK were carried out in 2006, 2009, and 2010, whereas for KBR only data from 2006 and 2010 are available. The 2006 and 2010 ALS data of both rock glaciers result from the same data acquisition campaigns (see Table 1). The average ALS point density of the individual ALS campaigns varies between 2.7 and 4.8 points per m^2.

Reference data: dGNSS

Differential global navigation satellite system (dGNSS) data are used to validate the vertical accuracy of the ALS-based DTMs as well as the calculated horizontal displacement rates. The dGNSS measurements were acquired in a well-established monitoring network (Schneider & Schneider 2001) of which four cross profiles at AHK and eleven fix points outside the rock glacier were included in our analysis. The locations of the dGNSS measurements (four cross profiles: L0 to L3 and the fix points) are given in Figure 1 and Figure 2.

Methods

Calculation of horizontal surface displacement

The image correlation software Imcorr is used to calculate horizontal surface displacements (Scambos et al. 1992). Imcorr has been widely applied to calculate flow velocities of glaciers using a variety of input data (Dowdeswell & Benham 2003, Giles et al. 2009). The software calculates displacement rates as a function of systematic changes in image digital numbers (DNs). The algorithm normalizes a reference chip and a larger search chip to a DN mean of zero and unity standard deviation prior to correlating the two chips (Scambos et al. 1992). The software uses raster images of two different dates as input and produces an output file consisting of the x- and y-coordinates (center pixel) of the moved reference chip, the displacement rates in x- and y-directions, as well as a correlation strength parameter.

As Imcorr uses raster images as input, the original ALS point clouds of 2006, 2009, and 2010 are interpolated to DTMs with 0.5 m raster resolution in a first step. Each raster cell is populated with the average value of all z-coordinates (height value) that spatially lie within that cell. As the horizontal ALS point spacing is very regular, more than 76% of all raster cells are populated without interpolating from neighboring cells; the remaining 24% are filled using a nearest-neighbor function. For each DTM, a shaded relief raster is calculated (azimuth

North-West, altitude 45°), which is then used as input for the image correlation. Imcorr was run with a reference chip of 16 x 16 cells, a search chip of 64 x 64 cells, and a moving window spacing of 1 cell.

Accuracy assessment

The accuracy of the calculated horizontal displacement rates is evaluated using dGNSS data. As the dGNSS measurements and ALS data acquisitions have not been carried out at the same dates (Table 1), the ALS-based displacement rates are adjusted to the time span between the dGNSS data acquisitions using

$$\overline{dALS}_{t1,t2} = ALS_{t1,t2} / \Delta tALS_{t1,t2} * \Delta tdGNSS_{t1,t2} \quad (1)$$

where $\overline{dALS}_{t1,t2}$ is the adjusted displacement rate [ma^{-1}] of the Imcorr results, $ALS_{t1,t2}$ is the displacement rate of the original Imcorr results, $\Delta tALS_{t1,t2}$ is the number of days between the ALS flight campaigns and $\Delta tdGNSS_{t1,t2}$ is the number of days between the dGNSS measurements. The time-adjusted Imcorr output point file and the interpolated displacement raster values are compared to the dGNSS displacement rates. For the generation of displacement rates, a trimmed mean interpolation function (search radius 2 m) was used. This allowed the removal of erroneous measurements (outliers).

For the 2009–2010 time period, 39 dGNSS measurements from the cross profiles L0 to L3 are used for validation. For the period 2006–2010, dGNSS data from L1 are not available and therefore only 28 reference measurements could be used. The vertical accuracy of the generated DTMs at AHK is determined using eleven dGNSS measurement sites (see Fig. 1). The eleven fix points are not influenced by any topographic changes.

Results and Discussion

Vertical accuracy of the DTMs

A comparison between the generated DTMs of AHK and the dGNSS heights at 11 fix points shows mean deviations of -0.02 m (std 0.15 m) for the 2006 DTM, 0.04 m (std 0.09 m) for 2009 DTM, and 0.09 m (std 0.09 m) for 2010 DTM. Thus, using the standard deviation as an accuracy measure, the vertical accuracy of all DTM heights is better than 0.15 m.

Accuracy of horizontal displacement rates

The mean deviations between the ALS-based displacement rates and the dGNSS results range between -0.10 m and 0.08 m and are relatively small. These values near zero indicate that no systematic respective over- underestimation of the velocity occurs. However, the standard deviations between 0.30 m and 0.51 m, as well as the average absolute deviation between 0.22 m and 0.39 m, are more appropriate to define the accuracy of the ALS-based displacement rates. In this study we use the standard deviation as the level of significance. Thus, for the one-year time period 2009–2010, displacement rates > 0.30 m exceed the level of significance. For the four-year time period 2006–2010, the level of significance is 0.50 m.

Table 2. Comparison between adjusted horizontal displacement rates from Imcorr (equation 1) and dGNSS (Imcorr – dGNSS).

Imcorr - dGNSS	Mean [m]	Amean [m]	Std [m]	Max [m]	Min [m]	RMS [m]	R^2
Pts. 09/10	-0.10	0.25	0.36	0.96	-1.28	0.37	0.92
Raster 09/10	-0.08	0.22	0.30	0.52	-0.91	0.30	0.94
Pts. 06/10	-0.19	0.39	0.51	1.09	-1.11	0.54	0.97
Raster 06/10	-0.12	0.34	0.50	1.27	-1.15	0.50	0.98

Mean: Mean deviation between dGNSS and Imcorr; Amean: average absolute deviation; Std: Standard deviation; Max/Min: Maximum/Minimum deviation; RMS: root mean square error; R^2: Coefficient of determination. In columns with "Pts." the adjusted Imcorr output points (equation 1) are compared to dGNSS; 2009-10 n=39, 2006-10 n=28.

All accuracy measures in Table 2 indicate that the accuracy of the 2009–2010 displacements is generally better than the accuracy for 2006–2010. Furthermore, it becomes obvious that the interpolation of the original Imcorr output point files to the raster maps improved the accuracy. This is due to the fact that outliers (e.g., local maxima and minima) are removed by the trimmed mean interpolation algorithm, and also due to averaging all values found in the search radius of 2 m to populate each raster cell.

As dGNSS data are only available for AHK, we also use the level of significance determined at AHK for the KBR data.

Surface elevation change of AHK

Surface elevation change rates > 0.5 m are identified in several areas of AHK. At the orographic right margin of the rock glacier, values >0.5 m are caused by creep processes that resulted in a downward transport of mass and expansion of AHK between 2006 and 2010 (Figs. 1 and 2). Distinct elongate-shaped alterations of positive and negative values occur on the main part of the rock glacier, especially between 2730 m and 2820 m at the orographic right side. They clearly result from advancing ridges and furrows. Between L0 and L1, at about 2500 m at the middle part of AHK, a sharp transition from areas with high surface elevation decrease and gain is evident. These areas correspond well with the area described by Haeberli & Patzelt (1982) and Schneider & Schneider (2001), where deep cross cracks occur as a consequence of local sliding of the rock glacier on the bedrock and increased tension in the permafrost body.

In general, the detected local surface elevation changes of AHK are caused by horizontal displacements of the creeping rock glacier. Regarding the entire rock glacier, an area-averaged mass loss is not detected. Therefore, the ice content of AHK seems to be well protected from surface energy input, and significant ice melt did not occur between 2006 and 2010.

Surface velocity of AHK

Individual surface velocity fields are detected for the time period 2006 to 2010 (Fig. 2). In general, the mean annual

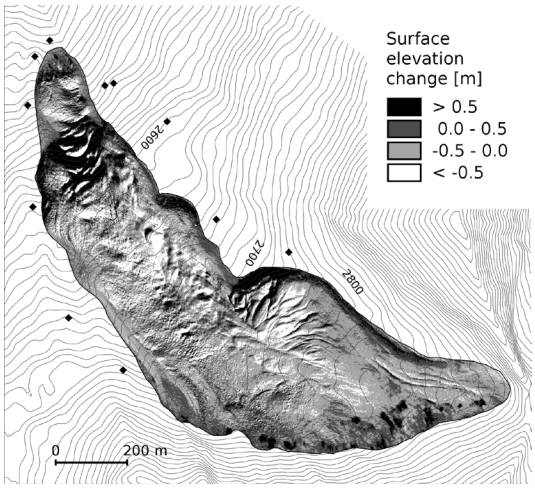

Figure 1. Surface elevation change of AHK between 2006 and 2010. Results based on DTM differencing with 0.5 m resolution. Black rhombus shows location of dGNSS fix points.

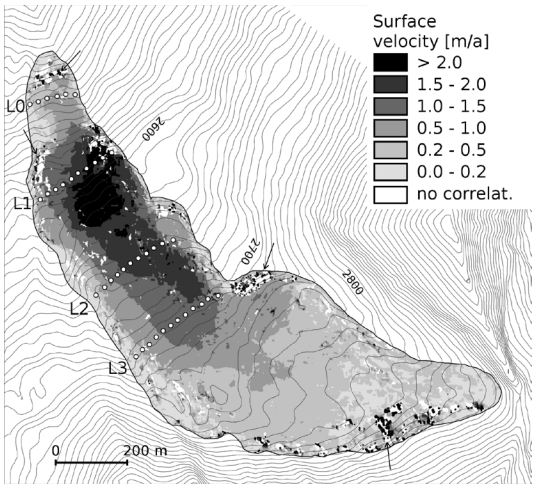

Figure 2. Mean annual surface velocity of AHK between 2006 and 2010. Results interpolated from Imcorr output. L0 to L3 (white circles) indicate location of dGNSS measurement points along 4 cross profiles. Arrows indicate areas with artifacts.

velocity increases gradually from < 0.2 ma^{-1} at the root zone to a maximum of > 2 ma^{-1} in the middle part of the rock glacier and at its orographic right side at about 2600 m. Maximum velocities correspond well with an increase of terrain steepness below 2640 m. Below 2560 m, the surface velocity decreases again, even though the terrain is still steep. A complete decoupling of the upper and lower part of AHK, as has been assumed by Haeberli & Patzelt (1982), cannot be found in the analysis of the 2006–2010 velocity fields. The velocity decrease between L1 and L0 is gradual rather than abrupt. However, the lowest part of AHK (around L0) is clearly influenced by other creep characteristics than the part above 2560 m (Figs. 1 and 2).

For some areas, no creep rates could be calculated because no correlations between the two input images are made by Imcorr. These areas occur either at steep lateral sides or in

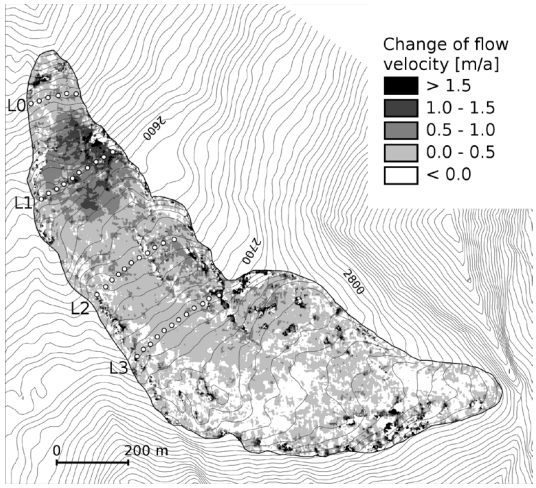

Figure 3. Changes in mean annual flow velocity between the time period 2006-2009 and 2009-2010.

fast creep steep areas. In these areas, the surface topography changes strongly due to rotation of boulders and surface instabilities. Several velocity artifacts occur (arrows in Fig. 2) that result from miss-matching of the two Imcorr input images. In most cases, they are spatially connected to areas where no correlation of the two images could be made. Such areas have to be excluded from interpretation.

Flow velocity changes of AHK

Between the 2006–2009 period and 2009–2010, a general velocity increase is detected. Comparing Figure 2 and Figure 3 shows that the absolute increase of surface velocity is highest for areas that initially show high mean annual velocities. The most significant acceleration on the order of 1.0–1.5 ma^{-1} occurs in the steep part of the rock glacier at the cross profile line L1. Velocity changes in that area have been discussed by Haeberli & Patzelt (1982) and Schneider & Schneider (2001). Most likely they do not present variations in internal creep characteristics but are a result of sliding at the base of the creeping permafrost body on the bedrock. Over large parts of the rock glacier, a velocity increase on the order of 0.0–0.5 ma^{-1} is observed, whereas toward the root zone slightly negative values are calculated. These values are near or below the level of significance of 0.3 m (cf. Table 2, Std Raster 09/10). Thus, considering the accuracy of the data and method, it cannot be stated that the velocity really decreased in the root zone of AHK.

Surface elevation change of KBR

DTM differencing of the KBR rock glacier indicates a mean surface lowering of -0.21 m between 2006 and 2010 (Fig. 4). Positive values, indicating an increase of surface elevation, are found at the margins of the rock glacier and result from the advance of the rock glacier lobe. Surface elevation increase > 0.6 m occurs at the front of the eastern lobe. Further positive values, between 0.0 m and 0.6 m, are identified in the areas of well-defined ridges as a result of the creep process and in the root zone. Surface elevation increase in the root zone might

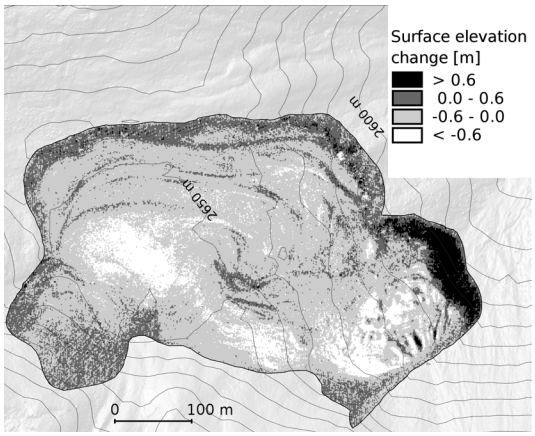

Figure 4. Surface elevation change of KBR between 2006 and 2010. Results based on DTM differencing with 0.5 m resolution.

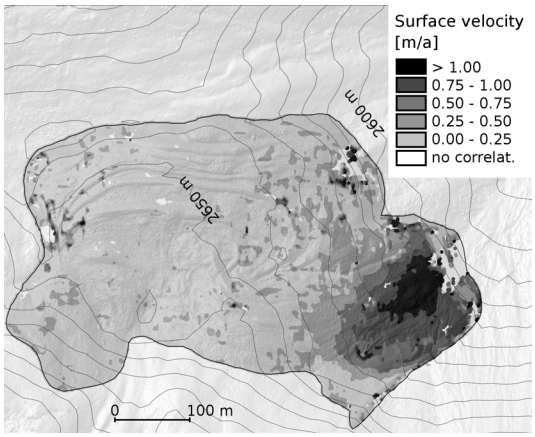

Figure 5. Mean annual surface velocity of KBR between 2006 and 2010. Results interpolated from Imcorr output.

result from debris input from the headwall area. The largest part of KBR shows surface elevation lowering in the order of 0.0 to -0.6 m, whereas surface lowering < -0.6 m is found at the fast creeping body and the central part of the western lobe.

Due to the fact that surface elevation losses are not balanced out by surface elevation gain, it can be concluded that KBR is in a degrading stage where ice melt occurs.

Surface velocity of KBR

The mean annual surface velocity between 2006 and 2010 of KBR ranges from areas with 0.00–0.25 ma^{-1} to areas with > 1.00 ma^{-1} (Fig. 5). A clear distinction in creep dynamics between a larger, slow-creeping western part and a smaller, faster-creeping eastern part is evident. Maximum velocities of > 1.00 ma^{-1} occur in the central part of the fast-creeping body and can be explained by a rather steep slope gradient of 15° compared to the flatter western part of KBR. Velocities gradually decline toward the orographic right margin and toward the main body orographic left.

Conclusion and Outlook

Horizontal displacements of the Hochebenkar and Kaiserberg rock glaciers could be calculated from multi-temporal ALS data. Comparisons between the ALS-based surface displacement raster and dGNSS data indicate an accuracy (standard deviation) of the calculated displacement rates of 0.3 m for the period 2009–2010 and 0.5 m (0.13 for an annual scale) for the period 2006–2010. As AHK is a very fast-creeping rock glacier, the data and method used are sufficient to achieve significant results for almost all parts of the rock glacier. However, a time span smaller than five years between the ALS data acquisition dates and raster resolution of 0.5 m might not be long enough to obtain significant results for slow-creeping rock glaciers.

For the AHK, a gradual increase of mean annual surface velocity from < 0.1 ma^{-1} at the root zone to > 2 ma^{-1} at the lower part (around 2600 m) was calculated over the period 2006–2010. Beside the class 0.0–0.2 m a^{-1}, all other velocity classes exceed the level of significance of 0.13 m for an annual scale. From 2600 m downward, the mean annual velocity gradually declined again. Comparing the period 2006–2009 with the period 2009–2010, a general increase of flow velocity is evident. Over large parts of AHK, the velocity increase is > 0.5 ma^{-1}, but increases of > 1.5 ma^{-1} also occur in areas with high initial flow velocities.

The KBR rock glacier showed two spatially distinct flow velocity patterns; a fast-creeping orographic right part (up to > 1 ma^{-1}) and a relatively slow-creeping left part (< 0.25 ma^{-1}).

In the case of AHK, permafrost creep is the most important factor governing local surface elevation changes. Conversely, the detected area-averaged surface lowering of KBR of -0.21 m is attributed to ice melt.

Future applications of ALS in rock glacier monitoring should focus on (1) the method's capability to quantify very slow-creeping permafrost, (2) the performance on rock glaciers with small changes of local surface topography (smooth surface), (3) the calculation of 3D displacements, and (4) area-wide quantification of rock glacier creep.

Acknowledgments

We thank the Tyrolean Government, the Austrian Climate and Energy Funds (C4AUSTRIA project, ACRP-A963633), and alpS – Centre of climate change adaption strategies (MUSICALS project) for the funding and provision of the ALS data. Furthermore, we thank H. Schneider, who provided the dGNSS data. The constructive comments of the two reviewers, Y. Buhler and R. Kenner, are much appreciated.

References

Baltsavias, E. 1999. Airborne laser scanning: basic relations and formulas. *ISPRS Journal of photogrammetry and remote sensing* 54: 199-214.

Barsch, D. 1996. *Rockglaciers. Indicators for the present and former geoecology in high mountain environments.* Springer-Verlag. Berlin.

Bauer, A., Paar, G., & Kaufmann, V. 2003. Terrestrial laser scanning for rockglacier monitoring. In: Phillips, M., Springman, S.M., Arenson, L.U. (Eds.), *Proceedings of the 8th international conference on permafrost.* Swets and Zeitlinger, Lisse, 1: 55-60.

Bollmann, E., Sailer, R., Briese, Ch., Stötter, J., & Fritzmann, P. 2010. Potential of airborne laser scanning for geomorphologic feature and process detection and quantification in high alpine mountains. *Zeitschrift für Geomorphologie* 55(Suppl. 2): 83-104.

Dowdeswell, J.A. & Benham, T.J. 2003. A surge of Perseibreen, Svalbard, examined using aerial photography and ASTER high resolution satellite imagery. *Polar research* 22(2): 373-383.

Giles, A.B., Massom, R.A., & Warner, R.C. 2009. A method for sub-pixel scale feature-tracking using Radarsat images applied to the Mertz glacier tongue, East Antarctica. *Remote sensing of environment* 113: 1691-1699.

Haeberli, W. 1982. Creep of mountain permafrost: Internal structure and flow of alpine rock glaciers. Mitteilungen der Versuchsanstalt für Wasserbau, *Hydrologie und Glaziologie ETH Zürich* 77: 1-142.

Haeberli, W. & Patzelt, G. 1982. Permafrostkartierung im Gebiet der Hochebenkar-Blockgletscher, Obergurgl, Ötztaler Alpen. *Zeitschrift für Gletscherkunde und Glazialgeologie* 18 (2): 127-150.

Haeberli, W., Hallet, B., Arenson, L., Elconin, R., Humlum, O., Kääb, A., Kaufmann, V., Ladanyi, B., Matsuoka, N., & Vonder Mühll, D. 2006. Permafrost creep and rock glacier dynamics. *Permafrost and periglacial processes* 17 (3): 189-214.

Harris, C., Arenson, L., Christiansen, H., Etzelmüller, B., Frauenfelder, R., et al. 2009. Permafrost and climate in Europe: Monitoring and modelling thermal, geomorphological and geotechnical responses. *Earth-science reviews* 92: 117-171.

Hodgsonn, M. & Bresnahan, P. 2004. Accuracy of airborne Lidar-derived elevation: Empirical assessment and error budget. *Photogrammetric engineering and remote sensing* 70(3): 331-339.

Kaufmann, V & Landstädter, R. 2002. Spatial-temporal analysis of the dynamic behaviour of the Hochebenkar rock glacier (Ötztal Alps, Austria) by means of digital photogrammetric methods. *Grazer Schriften der Geographie und Raumforschung* 37: 119-140.

Kaufmann, V & Landstädter, R. 2003. Quantitative analysis of rock glacier creep by means of digital photogrammetry using multi-temporal aerial photographs: two case studies in the Austrian Alps. In: Phillips, M., Springman, S.M., Arenson, L.U. (Eds.), *Proceedings of the 8th international conference on permafrost.* Swets and Zeitlinger, Lisse, 1: 525-530.

Kääb, A. & Weber, M. 2004. Development of transverse ridges on rock glaciers: Field measurements and laboratory experiments. *Permafrost and periglacial processes* 15: 379-391.

Kääb, A., Frauenfelder, R., & Roer, I. 2007. On the reaction of rockglacier creep to surface temperature variations. *Global and planetary change* 56: 172-187.

Kääb, A., Haeberli, W., & Gudmundsson, H. 1997. Analysing the creep of mountain permafrost using high precision aerial photogrammetry: 25 years of monitoring Gruben rock glacier, Swiss Alps. *Permafrost and periglacial processes* 8: 409-426.

Kääb, A., Kaufmann, V., Landstädter, R., & Eiken, T. 2003. Rock glacier dynamics: implications from high-resolution measurements of surface velocity fields. In: Phillips, M., Springman, S.M., Arenson, L.U. (Eds.), *Proceedings of the 8th international conference on permafrost.* Swets and Zeitlinger, Lisse, 1: 501-506.

Kääb, A., Isaksen, K., Eiken, T., & Farbot, H. 2002. Geometry and dynamics of two lobe-shaped rock glaciers in the permafrost of Svalbard. *Norsk geografisk tidsskrift* 56: 152-160.

Kenny, L.W. & Kaufmann, V. 2003. Estimation of rock glacier surface deformation using SAR interferometry data. *Geoscience and remote sensing* 41(6): 1512-1515.

Krainer, K. & Mostler, W. 2006. Flow velocities of active rock glaciers in the Austrian Alps. *Geografiska Annaler* 88 A (4): 267-280.

Roer, I., Kääb, A., & Dikau, R. 2005. Rockglacier kinematics derived from small-scale aerial photography and digital airborne pushbroom imagery. *Zeitschrift für Geomorphologie* 49(1): 73-87.

Scambos, T.A., Dutkiewitcz, M.J., Wilson, J.C., & Bindschadler, R.A. 1992. Application of image cross-correlation software to the measurement of glacier velocity using satellite data. *Remote sensing of environment* 42: 177-186.

Schneider, B. & Schneider, H. 2001. Zur 60jährigen Messreihe der kurzfristigen Geschwindigkeitsschwankungen am Blockgletscher im Äußeren Hochebenkar. *Zeitschrift für Gletscherkunde und Glazialgeologie* 37: 1-33.

Strozzi, T., Kääb, A., & Frauenfelder, R. 2004. Detecting and quantifying mountain permafrost creep from in-situ, airborne and spaceborn remote sensing methods. *International journal of remote sensing* 25(15): 2919-2931.

Vietoris, L. 1972. Über den Blockgletscher des Äußeren Hochebenkars. *Zeitschrift für Gletscherkunde und Glazialgeologie* 8 (1-2): 169-188.

Whalley, W.B. & Martin, H.E. 1992. Rock glaciers: II models and mechanics. *Progress in physical geography* 16: 127-186.